Phys Chem Minerals (2015) 42:303–308
DOI 10.1007/s00269-014-0720-y

ORIGINAL PAPER

Pressure-dependent Raman spectra of β-$Ca_3(PO_4)_2$ whitlockite

Shuangmeng Zhai · Xiang Wu · Weihong Xue

Received: 25 June 2014 / Accepted: 25 October 2014 / Published online: 4 November 2014

Abstract The pressure dependence of Raman spectra for whitlockite β-$Ca_3(PO_4)_2$ was investigated up to 18.0 GPa using a diamond-anvil cell at room temperature. The Raman frequencies of all observed bands for β-$Ca_3(PO_4)_2$ continuously increase with increasing pressure. The quantitative analysis of pressure dependence of Raman bands for the sample shows that the ν_3 asymmetric and ν_1 symmetric stretching vibrations are with the larger pressure coefficients (from 3.44 to 4.59 cm^{-1} GPa^{-1}) and that the ν_4 bending and ν_2 deforming vibrations are with the smaller pressure coefficients (from 1.46 to 3.12 cm^{-1} GPa^{-1}). Combined with previous result, the isothermal mode Grüneisen parameters of β-$Ca_3(PO_4)_2$ were calculated. The splitting of the PO_4 symmetric stretching ν_1 vibrations changes during compression and disappears around 15.4 GPa, which may be attributed to the evolution of PO_4 tetrahedra under high pressure.

Keywords Whitlockite · β-$Ca_3(PO_4)_2$ · High pressure · Raman spectra

S. Zhai (✉) · W. Xue
Key Laboratory of High-temperature and High-pressure Study of the Earth's Interior, Institute of Geochemistry, Chinese Academy of Sciences, Guiyang 550002, Guizhou, China
e-mail: zhaishuangmeng@vip.gyig.ac.cn

X. Wu
Key Laboratory of Orogenic Belts and Crustal Evolution, MOE, School of Earth and Space Sciences, Peking University, Beijing 100871, China

Introduction

The tricalcium phosphate [TCP, $Ca_3(PO_4)_2$] is one of the important phosphates. Many researchers, such as biologists, and inorganic and industrial chemists, are interested in this material since it is one of the most important biomaterials (Nurse et al. 1959; Rejda et al. 1977; Bigi et al. 1988; Elliott 1994) and it is with interesting luminescent properties (Sarver et al. 1961). TCP has four polymorphs of β-, α-, α′-, and γ-phase (Nurse et al. 1959; Murayama et al. 1986). The β-TCP is a resorbable phase and exhibits good biocompatibility (Jarcho et al. 1979; Kivrak and Tas 1998; Gibson et al. 2000), which has been widely used as a biocompatible material for bone replacement and for the coating of prosthetic implants as well as apatites (Elliott 1994). In fact, β-$Ca_3(PO_4)_2$ was initially labeled as whitlockite (Frondel 1941) and in rhombohedral structure (space group of $R3c$, $Z = 21$) (Gopal and Calvo 1972; Prewitt and Rothbard 1975; Dowty 1977; Yashima et al. 2003). Whitlockite was found as a common phosphate in lunar rocks and meteorites (Griffin et al. 1972; Delaney et al. 1984; Lundberg et al. 1988; Rojkovič et al. 1997; Anand et al. 2003; Ángeles et al. 2010; Xie et al. 2013).

Studies of the vibrational properties of β-TCP by means of Raman scattering measurement at ambient conditions have been reported (de Aza et al. 1997; Jillavenkatesa and Condrate 1998). The application of pressure usually has a large effect on the physical properties of materials. However, there is little work on the vibrational behavior of the β-TCP phase under compression.

In this paper, we report the first high-pressure micro-Raman spectroscopic study on the β-TCP up to 18.0 GPa using a diamond-anvil cell. The study has been performed over the frequency range from 300 to 1,200 cm^{-1}. The effect of pressure on the characteristic Raman active

internal PO_4^{3-} modes of β-TCP is analyzed and discussed in relation to the crystal structure.

Experimental

High-purity β-TCP was prepared by a solid-state reaction from $CaHPO_4$ and $CaCO_3$. Reagent-grade $CaHPO_4$ and $CaCO_3$ powders were mixed in the proportion corresponding to $Ca_3(PO_4)_2$ stoichiometry, and the mixture was ground for 2 h in an agate mortar and pressed into pellets with a diameter of 5 mm under uniaxial pressure of 30 MPa. The pellets were sintered at 1,300 K for 48 h to form a single phase of β-TCP. The sintered product was crushed and ground into powder and characterized by powder X-ray diffractometer. The X-ray pattern confirmed the formation of a single β-TCP phase.

The high-pressure Raman spectroscopic measurements using a four-pin modified Merrill–Basset diamond-anvil cell were taken at Bayerisches Geoinstitut, Universität Bayreuth. The experimental method used in this study was similar to a previous study (Zhai et al. 2010). A Re metal plate with an initial thickness of 260 μm was used as gasket. The central area of the plate was pre-indented to a thickness of about 30 μm, and a hole of 150 μm in diameter was drilled through it. The synthetic β-TCP and a tiny ruby sphere were loaded with the Ne pressure medium into the hole in the gasket. The experimental pressure was determined using the ruby fluorescence method (Mao et al. 1978), and the estimated error is within 0.5 GPa in this study. Micro-Raman spectra were recorded in backscattering geometry using Dilor X–Y spectrometer with a liquid nitrogen-cooled CCD detector, 50× objective, and confocal mode. The digital resolution is about 1 cm^{-1}. Excitation was performed adopting an argon-ion laser with a wavelength of 514.5 nm and a power of 0.786 W. The acquisition time of each spectrum was 90 s. The Raman shift of each band was obtained by Lorentzian curve fitting to get a reasonable approximation.

Results and discussion

The β-TCP has a rhombohedral structure belonging to the *R3c* space group with $Z = 21$. In the this structure, phosphorus atoms are located at three crystallographic sites and tetrahedrally coordinated by oxygen atoms, and calcium atoms occupy five sites from Ca(1) to Ca(5). The coordinated numbers for Ca atoms from Ca(1) to Ca(5) are 7, 8, 8, 3, and 6, respectively (Yashima et al. 2003). The crystal structure of β-TCP can be described by the two kinds of columns of A and B types along the *c*-axis (Dickens et al. 1974; Elliott 1994; Yashima et al. 2003). The A column is with the form of $–P(1)O_4–Ca(4)O_3–Ca(5)O_6–P(1)O_4–$, while the B column is of the form $–P(3)O_4–Ca(1)O_7–Ca(3)O_8–Ca(2)O_8–P(2)O_4–P(3)O_4–$. The B column is distorted and with a dense structure compared with the A column.

As described in previous study (de Aza et al. 1997), the factor group analysis of β-TCP yields 189 Raman active internal vibrations of PO_4^{3-}, including $7A_1 + 14E$ from the ν_1 symmetric stretching mode, $14A_1 + 28E$ R from the ν_2 deforming mode, $21A_1 + 42E$ from the ν_3 asymmetric stretching mode, and $21A_1 + 42E$ from the ν_4 bending mode. However, due to the low intensity and overlapping of a large number of internal vibrations, the number of observed Raman active bands is much less than 189. As shown in Fig. 1 and listed in Table 1, totally 13 Raman active internal vibrations of β-TCP were observed, including 4 vibrations of ν_2 deforming mode, 4 vibrations of ν_4 bending mode, 2 vibrations of ν_1 symmetric stretching mode, and 3 vibrations of ν_3 asymmetric stretching mode. The Raman spectrum was not analyzed by full range from 350 to 1,150 cm^{-1}, but by four separated ranges of 350–520, 520–660, 900–1,000, and 1,000–1,150 cm^{-1} using PeakFit Program. Therefore, the peaks can be located well. Though the number of observed Raman peaks was less than that reported by de Aza et al. (1997), the typical characterization is similar.

It is noted that the intensity of the internal PO_4 symmetric stretching mode (ν_1) located at 952 and 973 cm^{-1} was strongest among the Raman peaks. An obvious splitting of the ν_1 mode was observed, which is attributed to the effects of the distortions of the phosphate ions and the consequent spread of intratetrahedral bond lengths (de Aza et al. 1997). According to the high-resolution neutron powder diffraction results of β-TCP (Yashima et al. 2003), the P–O bond lengths of the PO_4 tetrahedra are from 1.510 to 1.574 Å with a variation of 0.064 Å. The averaged P–O bond lengths of $P(1)O_4$, $P(2)O_4$, and $P(3)O_4$ tetrahedra are 1.540, 1.538, and 1.535 Å, respectively. A longer bond length implies a weaker bond, i.e., smaller force constant and lower vibrational frequency according to Hooke's law. Therefore, the splitting of the ν_1 symmetric stretching mode is due to the different types of nonequivalent PO_4 tetrahedra.

The Raman spectra of β-TCP were collected up to 18.0 GPa at room temperature. Figure 2 shows the typical Raman spectra of β-$Ca_3(PO_4)_2$ at different pressures. At high pressures, a broadband appears in the Raman shift region of 700–800 cm^{-1}, which is attributed to the diamond and becomes weak with increasing pressure. The Raman bands of β-TCP gradually shift to higher frequency with increasing pressure. This is reasonable since the P–O bond lengths become shorter with increasing pressures and shorter bond lengths imply stronger bonds, i.e., larger force constant, and consequently higher vibrational frequency according to Hooke's law. The Raman bands of the PO_4

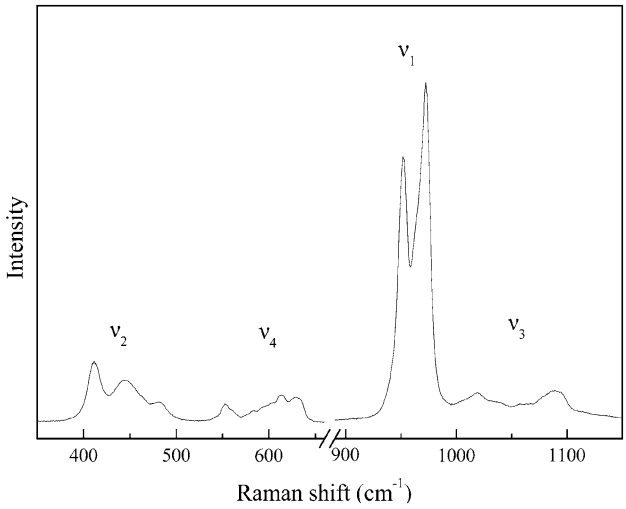

Fig. 1 Raman spectrum of β-$Ca_3(PO_4)_2$ at ambient conditions

Table 1 Constants determined in the expression: $\nu_P = \nu_{i0} + \beta P$ and mode Grüneisen parameter (γ_{iT}) at room temperature for β-$Ca_3(PO_4)_2$

Modes	ν_0	ν_{i0}	β	R^2	γ_{iT}
ν_3	1,088	1,088.5 (4)	4.59 (8)	0.998	0.335
	1,036	1,038.8 (17)	4.53 (24)	0.980	0.347
	1,019	1,018.2 (6)	3.50 (11)	0.993	0.273
ν_1	973	972.1 (9)	3.44 (12)	0.988	0.281
	952	952.9 (10)	3.87 (13)	0.989	0.323
ν_4	630	630.3 (11)	2.33 (15)	0.965	0.294
	614	613.9 (11)	1.90 (14)	0.951	0.246
	590	594.3 (13)	1.82 (17)	0.923	0.243
	554	552.4 (8)	1.46 (10)	0.959	0.210
ν_2	483	484.1 (11)	3.12 (14)	0.981	0.512
	461	458.8 (11)	2.81 (15)	0.976	0.487
	444	440.4 (12)	2.33 (16)	0.959	0.421
	411	410.0 (8)	2.50 (11)	0.983	0.485

ν_P and ν_{i0} are in cm^{-1} and β is in cm^{-1} GPa^{-1}. ν_0 was observed frequency (in cm^{-1}) at ambient conditions. R^2 is the correlation coefficient. Grüneisen parameter γ_{iT} was calculated with isothermal bulk modulus of $K_0 = 79.5$ GPa reported by Zhai and Wu (2010)

internal modes remain reasonably distinguishable before 15.4 GPa, where the splitting of the PO_4 symmetric stretching ν_1 vibrations disappears and the two highest intensity bands merge into a single peak, as illustrated in Fig. 2. The pressure dependence of the PO_4 internal vibrational modes was determined using the data before 15.4 GPa.

Figure 3a shows the vertical enlarged Raman spectra between 380 and 680 cm^{-1}. Although the two peaks around 450 cm^{-1} are not easy to distinguish at ambient pressure, it is clear that four peaks are suitable for fitting in the range of 380–530 cm^{-1}, especially at high-pressure conditions. In the range of 1,000–1,150 cm^{-1}, nine peaks were reported

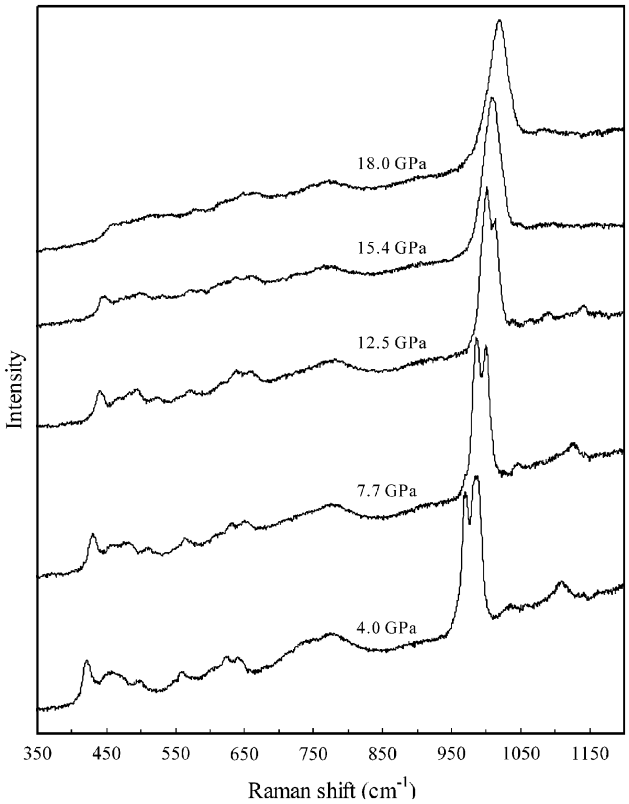

Fig. 2 Typical Raman spectra of β-$Ca_3(PO_4)_2$ at high pressures and room temperature. The band around 775 cm^{-1} is ascribed to the diamond anvil

by de Aza et al. (1997). However, fewer peaks can be distinguished from the Raman spectrum at ambient pressure in this study. The vertical enlarged Raman spectra between 1,000 and 1,150 cm^{-1} are shown in Fig. 3b. Here, three peaks were adopted to fit the spectra in the range of 1,000–1,150 cm^{-1}. It is noted that below 10 GPa the three peaks can be clearly located. Therefore, for the ν_3 asymmetric stretching mode, only data below 10 GPa were used for quantitative calculation.

Figure 4 presents the Raman shift versus pressure plot of β-TCP. It is obvious that the frequencies of phosphate modes for β-TCP vary linearly and continuously with pressure, implying that β-TCP is stable at room temperature through this pressure range. This is contrast with the behavior of β-TCP at high-temperature and high-pressure conditions (e.g., 950 °C and 4 GPa), where β-TCP transfers to γ-TCP (Roux et al. 1978; Murayama et al. 1986; Zhai et al. 2014). The pressure coefficients of PO_4 modes (Table 1) indicate that ν_3 and ν_1 bands in the higher-frequency region are more sensitive to pressure compared with the ν_4 and ν_2 bands in the lower-frequency region. In fact, the average pressure coefficients of ν_3 and ν_1 modes are 4.21 and 3.65 cm^{-1} GPa^{-1}, respectively, whereas the

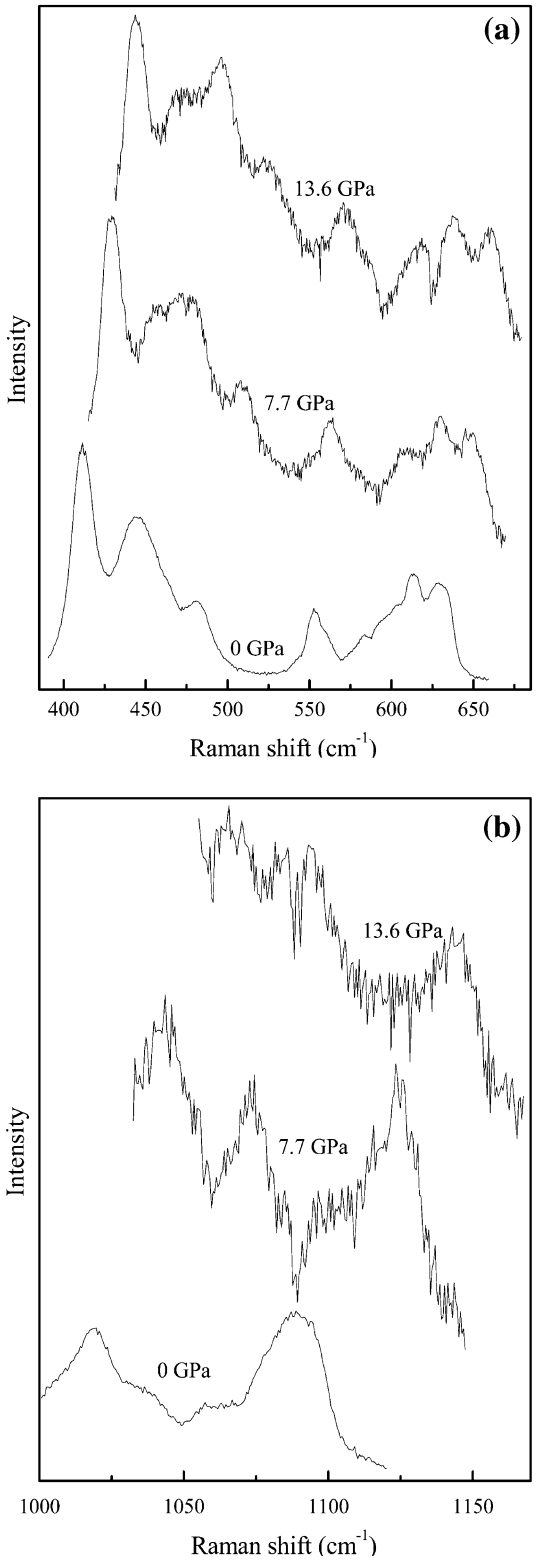

Fig. 3 Vertical enlarged Raman spectra of β-$Ca_3(PO_4)_2$ in the range of 380–530 cm^{-1} (**a**) and 1,000–1,170 cm^{-1} (**b**) at selected pressures and room temperature

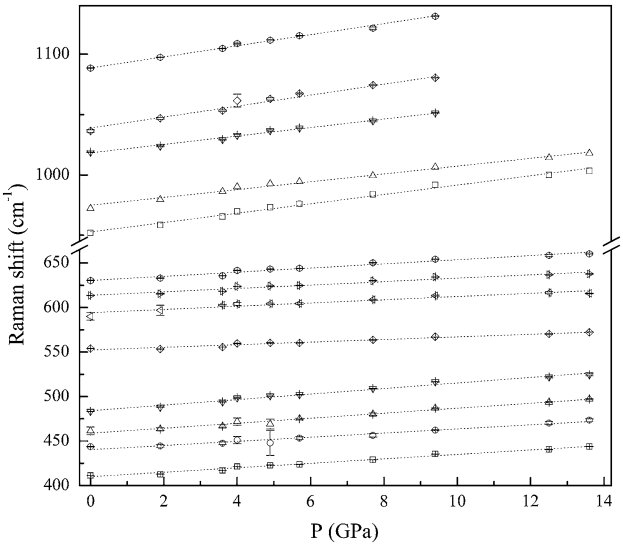

Fig. 4 Pressure dependence of the Raman bands of β-$Ca_3(PO_4)_2$ at room temperature

average pressure coefficients for ν_4 and ν_2 are 1.88 and 2.69 cm^{-1} GPa^{-1}, respectively.

The pressure coefficients of different Raman modes can be used to obtain the Grüneisen parameters which are extensively required in theoretical calculations. The Grüneisen parameter for each mode was calculated following the equation (Grüneisen 1912):

$$\gamma_{iT} = (\delta \nu_i / \delta P) K / \nu_i$$

where ν_i is the frequency of the i-th mode, K is the bulk modulus. We used a zero pressure isothermal bulk modulus, K_0 of 79.5 GPa (Zhai and Wu 2010). The Grüneisen parameters are also listed in Table 1. The average value for the mode Grüneisen parameters of the bands associated to phosphate group vibrations is 0.343, which is comparable with the values of other phosphates, such as fluorapatite and tuite (Williams and Knittle 1996; Comodi et al. 2001a; Zhai et al. 2010). The bulk thermochemical Grüneisen parameter, which is equal to $\alpha KV/C_v$ (where α is the thermal expansion, K is the bulk modulus, V is the molar volume, and C_v is the volume constant heat capacity), is not available for β-TCP due to the lack of precise thermal expansion. However, for incompressible oxide compounds without polymerized tetrahedra, the bulk Grüneisen parameters are usually in the range from 0.8 to 2 (Shankland and Bass 1988). Actually, the evolution of the tetrahedral modes is not representative of the structural evolution on the whole. It is noted that the external modes including the vibrations associated to the calcium polyhedra can strongly

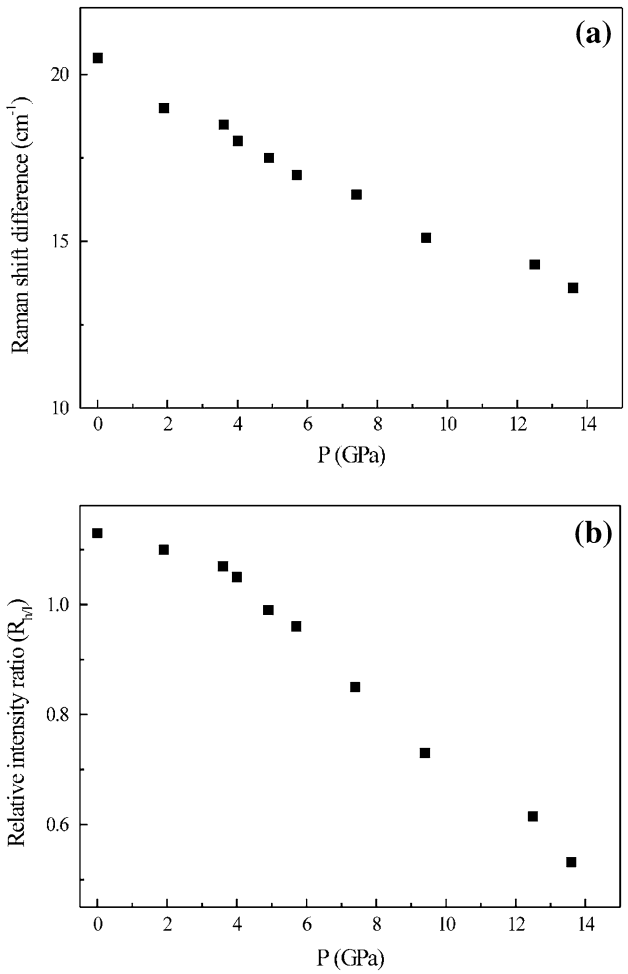

Fig. 5 The Raman shift difference (**a**) and relative intensity ratio (**b**) of splitting ν_1 symmetric stretching vibration at different pressures and room temperature

affect the bulk Grüneisen parameter, because the behavior of a Ca–O polyhedron is much less rigid than that of the PO_4 tetrahedron under high pressure (Comodi et al. 2001a). Therefore, for β-TCP and other phosphates including tuite and fluorapatite, the relatively low average value of the PO_4 mode Grüneisen parameters indicates that the lattice modes and vibrations related to Ca^{2+} displacements must considerably largely contribute to the bulk thermochemical Grüneisen parameter than the PO_4 vibrations.

As mentioned above, the two highest PO_4 symmetric stretching ν_1 vibrations approach and nearly merge into a single peak during compression. Indeed, at pressure of 15.4 GPa, it is difficult to resolve the two components of the ν_1 symmetric stretching mode. However, it does not indicate a phase change combined with the result of X-ray diffraction measurement in previous study (Zhai and Wu 2010). The decreasing splitting of ν_1 symmetric stretching mode in β-TCP is different from that of fluorapatite which shows decreasing splittings of ν_3 asymmetric stretching and ν_4 bending modes (Williams and Knittle 1996; Comodi et al. 2001a).

The Raman shift difference of splitting bands continuously decreases with increasing pressure, as shown in Fig. 5a. The reason is that the local crystal field surrounding the PO_4 groups deviates less from tetrahedral symmetry with increasing pressure. The intensity of high-frequency band (i.e., 973 cm^{-1} at ambient conditions) decreases and low-frequency band (i.e., 952 cm^{-1} at ambient conditions) increases during compression. The Raman intensity ratio of high-frequency band to low-frequency band ($R_{h/l}$) at different pressure is plotted in Fig. 5b. It is obvious that the $R_{h/l}$ decreases continuously with compression. The intensity of Raman band was affected by polarizability derivatives of PO_4. Therefore, the polarizability derivatives of PO_4 corresponding to both high-frequency and low-frequency vibrations of symmetric stretching ν_1 mode change during compression, which might cause that the variations of the P–O bond lengths and bond angles of the PO_4 tetrahedra in the β-TCP structure become small and disappear at high pressure. There is no information about the evolution of PO_4 tetrahedra in the crystal structure of β-TCP under high pressure. Previous study shows that in fluorapatite, although the average P–O bond length decreases with increasing pressure, some P–O bond lengths decrease and then increase during compression (Comodi et al. 2001b). There is only one P atom in the crystal structure of fluorapatite, but three P atoms in β-TCP. Therefore, the variations of PO_4 tetrahedron in β-TCP are much more complicated than that in fluorapatite. It is surmisable that the changes of PO_4 tetrahedra in β-TCP are highly complex. Crystal structure of β-TCP is required under high pressure in the future.

Conclusions

The Raman spectra of synthetic β-$Ca_3(PO_4)_2$ up to 18.0 GPa at room temperature have been observed and analyzed in the region of 300–1,200 cm^{-1}. The Raman frequencies of all observed vibrations continuously and linearly increase with increasing pressure. The pressure coefficients of the PO_4 internal modes range from 1.46 to 4.59 cm^{-1} GPa^{-1} and the calculated isothermal mode Grüneisen parameters vary from 0.210 to 0.512, yielding an average mode Grüneisen parameter of 0.343. A splitting of the ν_1 symmetric stretching mode of PO_4 decreases with compression and disappears around 15.4 GPa, which probably is due to the change of PO_4 tetrahedra at high pressure.

Acknowledgments The authors thank Prof. T. Tsuchiya for his editorial handling. Critical comments and suggestion from two anonymous reviewers are helpful to improve the manuscript. This work was

supported by National Natural Science Foundation of China (Grant nos. 41372040 and 41202020).

References

Anand M, Taylor LA, Neal CR, Snyder GA, Patchen A, Sano Y, Terada K (2003) Petrogenesis of lunar meteorite EET 96008. Geochim Cosmochim Acta 67:3499–3518

Ángeles S, Reyes AM, Macías C, Ortega F (2010) Mineralogy of the Pacula meteorite by electron microprobe analysis. Acta Microsc 19:44–50

Bigi A, Compostella L, Fichera AM, Foresti E, Gazzano M, Ripamonti A, Roveri N (1988) Structural and chemical characterization of inorganic deposits in calcified human mitral-valve. J Inorg Biochem 34:75–82

Comodi P, Liu Y, Frezzotti ML (2001a) Structural and vibrational behaviour of fluorapatite with pressure. Part II: in situ micro-Raman spectroscopic investigation. Phys Chem Minerals 28:225–231

Comodi P, Liu Y, Zanazzi PF, Montagnoli M (2001b) Structural and vibrational behaviour of fluorapatite with pressure. Part I: in situ single-crystal X-ray diffraction investigation. Phys Chem Minerals 28:219–224

de Aza PN, Santos C, Pazo A, de Aza S, Cuscó R, Artús L (1997) Vibrational properties of calcium phosphate compounds. 1. Raman spectrum of β-tricalcium phosphate. Chem Mater 9:912–915

Delaney JS, O'Neill C, Prinz M (1984) Phosphate minerals in eucrites. Lunar Planet Sci 15:208–209

Dickens B, Schroeder LW, Brown WE (1974) Crystallographic studies of the role of Mg as a stabilizing impurity in β-$Ca_3(PO_4)_2$. The crystal structure of pure β-$Ca_3(PO_4)_2$. J Solid State Chem 10:232–248

Dowty E (1977) Phosphate in Angra dos Reis: structure and composition of the $Ca_3(PO_4)_2$ minerals. Earth Planet Sci Lett 35:347–351

Elliott JC (1994) Structure and chemistry of the apatites and other calcium orthophosphates. Elsevier, Amsterdam

Frondel C (1941) Whitlockite: a new calcium phosphate $Ca_3(PO_4)_2$. Am Miner 26:145–152

Gibson IR, Rehman I, Best SM, Bonfield W (2000) Characterization of the transformation from calcium-deficient apatite to β-tricalcium phosphate. J Mater Sci Mater Med 11:533–539

Gopal R, Calvo C (1972) Structure relationship of whitlockite and β-$Ca_3(PO_4)_2$. Nat Phys Sci 237:30–32

Griffin W, Åmli R, Heier KS (1972) Whitlockite and apatite from lunar rock 14310 and from ÖdegÅrden, Norway. Earth Planet Sci Lett 15:53–68

Grüneisen E (1912) Theorie des festen zustandes einatomiger element. Ann Physik 12:257–306

Jarcho M, Salsbury RL, Thomas MB, Doremus RH (1979) Synthesis and fabrication of beta-tricalcium phosphate (whitlockite) ceramics for potential prosthetic applications. J Mater Sci 14:142–150

Jillavenkatesa A, Condrate RA (1998) The infrared and Raman spectra of β- and α-tricalcium phosphate ($Ca_3(PO_4)_2$). Spectrosc Lett 31:1619–1634

Kivrak N, Tas AC (1998) Synthesis of calcium hydroxyapatite-tricalcium phosphate (HA-TCP) composite bioceramic powders and their sintering behavior. J Am Ceram Soc 81:2245–2252

Lundberg LL, Crozaz G, McKay G, Zinner E (1988) Rare earth element carriers in the Shergotty meteorite and implications for its chronology. Geochim Cosmochim Acta 52:2147–2163

Mao HK, Bell PM, Shaner JW, Steinberg DJ (1978) Specific volume measurements of Cu, Mo, Pd and Ag and calibration of the ruby R_1 fluorescence pressure gauge from 0.06 to 1 Mbar. J Appl Phys 49:3276–3283

Murayama JK, Nakai S, Kato M, Kumazawa M (1986) A dense polymorph of $Ca_3(PO_4)_2$: a high pressure phase of apatite decomposition and its geochemical significance. Phys Earth Planet Inter 44:293–303

Nurse RW, Welch JH, Gutt W (1959) High-temperature phase equilibria in the system dicalcium silicate–tricalcium phosphate. J Chem Soc 1077–1083

Prewitt CT, Rothbard DR (1975) Crystal structures of meteoritic and lunar whitlockites. Lunar Planet Sci 6:646–648

Rejda BV, Peelen JGJ, de Groot K (1977) Tricalcium phosphate as a bone substitute. J Bioeng 1:93–96

Rojkovič I, Siman P, Porubčan V (1997) Rumanová H5 chondrite, Slovakia. Meteorit Planet Sci 32:A151–A153

Roux P, Lowor D, Bonel G (1978) Sur une novella forme cristallite du phosphate tricalcique. C R Acad Paris Ser C 286:549–551

Sarver JF, Hoffman MV, Hummel FA (1961) Phase equilibria and tin-activated luminescence in strontium orthophosphate systems. J Electrochem Soc 108:1103–1110

Shankland TJ, Bass JD (1988) Elastic properties and equations of state. American Geophysical Union, Washington, DC

Williams Q, Knittle E (1996) Infrared and Raman spectra of $Ca_5(PO_4)_3F_2$-fluorapatite at high pressures: compression-induced changes in phosphate site and Davydov splittings. J Phys Chem Solids 57:417–422

Xie X, Zhai S, Chen M, Yang H (2013) Tuite, γ-$Ca_3(PO_4)_2$, formed by chlorapatite decomposition in a shock vein of the Suizhou L6 chondrite. Meteorit Planet Sci 48:1515–1523

Yashima M, Sakai A, Kamiyama T, Hoshikawa A (2003) Crystal structure analysis of β-tricalcium phosphate $Ca_3(PO_4)_2$ by neutron powder diffraction. J Solid State Chem 175:272–277

Zhai S, Wu X (2010) X-ray diffraction study of β-$Ca_3(PO_4)_2$ at high pressure. Solid State Commun 150:443–445

Zhai S, Wu X, Ito E (2010) High-pressure Raman spectra of tuite, γ-$Ca_3(PO_4)_2$. J Raman Spectrosc 41:1011–1013

Zhai S, Akaogi M, Kojitani H, Xue W, Ito E (2014) Thermodynamic investigation on β- and γ-$Ca_3(PO_4)_2$ and the phase equilibria. Phys Earth Planet Inter 228:144–149